Molecular Catalysis 443 (2017) 209–219

Contents lists available at ScienceDirect

Molecular Catalysis

journal homepage: www.elsevier.com/locate/mcat

Editor's choice paper

Hydrogen bond donor functionalized dioxido-molybdenum(VI) complexes as robust and highly efficient precatalysts for alkene epoxidation

Niklas Zwettler, Jörg A. Schachner, Ferdinand Belaj, Nadia C. Mösch-Zanetti *

Institute of Chemistry, Inorganic Chemistry, University of Graz, Schubertstrasse 1, 8010 Graz, Austria

ARTICLE INFO

Article history:
Received 21 March 2017
Received in revised form
29 September 2017
Accepted 30 September 2017

Keywords:
Hydrogen bonds
Molybdenum
Epoxidation
Aminoamides
Homogeneous catalysis

ABSTRACT

The synthesis of four novel, tridentate aminophenolate ligands **HL1**-**HL4**, bearing amide functionalities is reported. Reaction of these ligands with a dioxido molybdenum(VI) precursor led, depending on the choice of solvent, to mononuclear complexes of the type $[MoO_2\mathbf{L}(OMe)]$ (**2**, **4**, **6**) or dinuclear complexes $[\{MoO_2\mathbf{L}\}_2(\mu\text{-}O)]$ (**1**, **3**, **5**, **7**), containing one facially, tridentate ONO-ligand per metal center. This synthetic discrimination between dinuclear and mononuclear complexes allows for a comparison between structures and reactivity. Complexes **1**-**7** were found to be highly active catalysts in the epoxidation of several internal and terminal alkenes. With *tert*-butyl hydroperoxide (TBHP) as oxidant, precatalyst loadings of 0.0005 mol% (5 ppm) could be realized leading to turnover numbers of up to 110000. The precatalysts also allowed for the use of hydrogen peroxide (0.1 mol% precatalyst) as oxidant as well as various alcohols as "green" solvents, such as ethanol or even *tert*-butanol (usually an inhibitor of epoxidation).

1. Introduction

The relative ease of ring-opening reactions, and thus the broad variety of possible follow-up products, makes epoxides very important intermediates in chemical synthesis [1–4]. One of the main synthetic route to epoxides is the oxidation of olefins. Different approaches exist for such a transformation, including the use of stoichiometric amounts of organic peracids as well as hetero- and homogeneous catalytic approaches [4,5]. Homogeneous catalytic protocols usually allow for mild conditions and often employ high valent metal-oxido complexes as precatalysts [3,6]. In the industrial production of propylene oxide via the Arco/Halcon process, such a protocol is realized with molybdenum and tungsten complexes as well as alkyl hydroperoxides as oxidants [1,7]. With the prospect to develop environmentally more friendly processes, the use of non-toxic, earth-abundant metals such as molybdenum is of key interest [8]. Especially mononuclear molybdenum(VI) dioxido complexes have proven to be highly active and selective precatalysts for the epoxidation of internal aliphatic olefins [9–11], recently the substrate scope could to some extent be expanded to terminal olefins [12,13]. Furthermore, the use of environmentally benign solvents as well as oxidants remains a major objective [14].

Initially, our research interest in high valent molybdenum compounds focused on oxygen atom transfer as well as the activation of molecular oxygen [15]. We then started to examine the catalytic behavior of the involved molybdenum complexes in the oxidation of olefins. In an endeavor to develop "greener" and more efficient catalytic protocols, our group tested several mono- and dinuclear dioxidomolybdenum(VI), and subsequently also mononuclear oxidorhenium(V) complexes for their capability of catalytic epoxidation of olefins as well as catalytic aerobic oxidation reactions. Whereas the investigated oxidorhenium(V) complexes were robust and in part allowed for the use of hydrogen peroxide as oxidant, they were limited to cyclooctene as substrate [16]. Dioxidomolybdenum systems on the other hand were able to catalyze the oxidation of a broad scope of substrates, albeit with varying selectivities [9,11,17,18]. Especially the use of bidentate Schiff-base ligands with donor sites led to very selective precatalysts [19]. Inspired by the work of Borovik and coworkers [20], we expanded our library of iminophenolate ligands by introducing amide functionalities as hydrogen bond donors and investigated their coordination chemistry with the dioxidomolybdenum(VI) fragment, finding unusual C—C and C—N coupling reactions at the metal center [21]. To inhibit such bond formation reactions but retain the structure of the ligands, we decided to investigate the derived aminophenolate derivatives, accessible via reduction of the imine C=N bond [18].

* Corresponding author.
E-mail address: nadia.moesch@uni-graz.at (N.C. Mösch-Zanetti).

http://dx.doi.org/10.1016/j.mcat.2017.09.036
2468-8231/

Herein we present the synthesis of four aminophenolate ligands featuring amide substituents with varying NH acidity by hydrogenation of the respective iminophenolates with Pd/C—H_2 or $NaBH_4$. The higher flexibility of those aminophenolate ligands leads to a monoanionic tridentate facial ONO coordination mode resulting in mono- and dinuclear dioxidomolybdenum(VI) complexes of the general formulas [{MoO_2**L**}$_2$(μ-O)] and [MoO_2**L**(OMe)]. The dinuclear complexes are structurally closely related to previously reported complexes, with the additional amide functionalities being of crucial difference [18]. A further important aspect of the system disclosed herein is the fact that both mono- and dinuclear complexes are formed depending on the reaction conditions, thus allowing for a direct comparison of their reactivity. The complexes were found to exhibit exceptionally high activity and functional group tolerance in the catalytic epoxidation of various alkene substrates with TBHP. This is in stark contrast to previously reported structural analogs[18] surpassing the activity of homogeneous epoxidation precatalysts known to date without additional hydrogen bond donors [9,12,22]. In addition we disclose herein the catalytic activity using H_2O_2 as oxidant as well as the use of environmentally benign alcoholic solvent [23].

2. Experimental section

2.1. General

Unless specified otherwise, experiments were performed under inert conditions using standard Schlenk equipment. Commercially available chemicals were purchased from Sigma–Aldrich and used as received. No further purification or drying operations have been performed. The metal precursor [MoO_2(acac)$_2$] [24] was synthesized according to known procedures. The used primary amines 2-amino-*N*-(*tert*-butyl)acetamide and 2-amino-*N*-phenylacetamide were synthesized according to a previously disclosed procedure [21]. Solvents were purified via a Pure–Solv MD–4–EN solvent purification system from Innovative Technology, Inc. Methanol was refluxed over activated magnesium for at least 24 h and then distilled prior to use. The ^{1}H, ^{13}C and HSQC NMR spectra were recorded on a Bruker Optics instrument at 300/75 MHz. Peaks are denoted as singlet (s), broad singlet (bs), doublet (d), doublet of doublets (dd), triplet (t), pseudo–doublet ("d"), pseudo–triplet ("t") and multiplet (m). Used solvents and peak assignment are mentioned at the specific data sets. HR-MS (ESI$^+$) measurements were performed at the University of Graz, Department of Analytical Chemistry using a Thermo Scientific Q-Exactive mass spectrometer in positive ion mode, the used solvent was acetonitrile. Peaks are denoted as cationic mass peaks, and the unit is the according ions mass/charge ratio. For dinuclear compounds the denoted mass peak corresponds to the highest found intensity, full calculated and found isotopic patterns are provided within the supporting information. Gas chromatography mass spectroscopy (GC–MS) measurements have been performed with an Agilent 7890A gas chromatograph (column type Agilent 19091J–433), coupled to an Agilent 5975C mass spectrometer. Samples for infrared spectroscopy were measured on a Bruker Optics ALPHA FT–IR Spectrometer. IR bands are reported with wavenumber (cm^{-1}) and intensities (s, strong; m, medium; w, weak). All elemental analyses were measured at the Technical University of Graz, Institute of Inorganic Chemistry using a Heraeus Vario Elementar automatic analyzer.

2.2. Catalytic epoxidation

A Heidolph Parallel Synthesizer 1 was used for all experiments. In a typical epoxidation experiment an aliquot of a stock solution of the respective precatalyst was stirred in 0.5 mL of the respective solvent and substrate was added. Mesitylene was used as internal standard. After the experiment temperature was reached the respective oxidant was added to start the reaction and samples for GC–MS measurements were withdrawn at given time intervals. GC samples were quenched with MnO_2, diluted with ethyl acetate and measured. Gas chromatography mass spectroscopy (GC–MS) measurements have been performed with an Agilent 7890 A gas chromatograph (column type, Agilent 19091J–433), coupled to an Agilent 5975C mass spectrometer. All yields obtained by GC have an esd of ±5%.

2.3. X–ray diffraction analyses

Single–crystal X–ray diffraction analyses were measured on a BRUKER–AXS SMART APEX II diffractometer equipped with a CCD detector. All measurements were performed using monochromatized Mo K_α radiation from an Incoatec microfocus sealed tube at 100 K (cf. Table S1). Absorption corrections were performed semi–empirical from equivalents. Structures were solved by direct methods (SHELXS–97) [25] and refined by full–matrix least–squares techniques against F^2 (SHELXL–2014/6) [25]. CCDC 1532978-1532983 contain the supplementary crystallographic data for this paper. These data can be obtained free of charge from The Cambridge Crystallographic Data Centre via www.ccdc.cam.ac.uk/data_request/cif. Full experimental details for single–crystal X–ray diffraction analyses of all compounds are provided in the SI.

2.4. Ligand synthesis

All ligands are stable towards air and moisture. They can be stored at ambient conditions for several weeks without decomposition.

2.5. Synthesis of N-(tert-*butyl*)-2-((2-*hydroxybenzyl*)*amino*)*acetamide (HL1)*

For the synthesis of **HL1**, 1 equiv. of 2-amino-*N*-(*tert*-butyl)acetamide [21] (1.75 g, 13.5 mmol) as well as 0.2 g of Pd/C (5 wt% Pd) were added to a solution of 1 equiv. of salicylic aldehyde (1.64 g, 13.5 mmol) in 80 mL of MeOH. The resulting dark-yellowish clouded solution was subsequently stirred at 50 °C in a pressure reactor under H_2 atmosphere (5 atm) for 24 h. The reaction solution was subsequently filtered and the reddish filtrate evaporated *in vacuo*. The crude reddish oily solid was purified via column chromatography on silica gel (ethyl acetate/cyclohexane gradient from 20% to 100% ethyl acetate) to give **HL1** as off-white solid (2.05 g, 65%). ^{1}H NMR (300 MHz, (CD_3)$_2$SO, 25 °C, OH & amine NH obscured) δ: 7.51 (bs, 1H, NH), 7.09-7.04 (m, 2H, ArH), 6.76-6.70 (m, 2H, ArH), 3.66 (s, 2H, CH_2), 3.02 (s, 2H, CH_2), 1.25 (s, 9H, *t*Bu) ppm; ^{13}C NMR (75 MHz, (CD_3)$_2$SO, 25 °C) δ: 169.95 (C=O), 156.47 (Ar-O), 129.24, 128.00, 124.95, 118.60, 115.19 (Ar), 51.39, 49.84, 49.33 (2x CH_2, q-*t*Bu), 28.51 (*t*Bu) ppm; HR-MS: (ESI$^+$) *m*/*z* [M+H]$^+$ calcd. for $C_{13}H_{20}O_2N_2$: 273.1598, found: 237.1594; IR (ATR, cm^{-1}) $\tilde{\nu}$: 1591 (m), 1537 (m), 1453 (m), 1391 (w), 1251 (w), 1224 (m), 754 (s), 435 (w);

2.6. Synthesis of N-(tert-*butyl*)-2-((3,5-*di*-tert-*butyl*-2-*hydroxybenzyl*)*amino*)*acetamide (HL2)*

For the synthesis of **HL2**, 1.1 equiv. of 2-amino-*N*-(*tert*-butyl)acetamide [21] (1.68 g, 12.9 mmol) as well as 0.5 g of Pd/C (5 wt% Pd) were added to a solution of 1 equiv. of 3,5-di-*tert*-butyl-2-hydroxybenzaldehyde (2.75 g, 11.7 mmol) in 100 mL of MeOH. The resulting yellowish clouded solution was subsequently stirred

at 50 °C in a pressure reactor under H_2 atmosphere (5 atm) for 24 h. The reaction solution was subsequently filtered and the pale violet filtrate evaporated *in vacuo*. The crude pale violet powder was purified via column chromatography on silica gel (ethyl acetate/cyclohexane gradient from 20% to 100% ethyl acetate) to give **HL2** as white solid (2.69 g, 66%). ^{1}H NMR (300 MHz, $(CD_3)_2SO$, 25 °C) δ: 11.44 (bs, 1H, OH), 7.53 (bs, 1H, NH), 7.08 (d, 1H, ArH), 6.84 (d, 1H, ArH), 3.78 (s, 2H, CH_2), 3.25 (bs, 1H, NH), 3.09 (s, 2H, CH_2), 1.35 (s, 9H, *t*Bu), 1.26 (s, 9H, *t*Bu), 1.22 (s, 9H, *t*Bu) ppm; ^{13}C NMR (75 MHz, $(CD_3)_2SO$, 25 °C) δ: 169.24 (C=O), 154.29 (Ar-O), 139.35, 134.46, 123.21, 122.49, 121.67 (Ar), 51.87, 50.17 (CH_2), 50.11, 34.42, 33.74 (q-*t*Bu), 31.55, 29.54, 28.55 (*t*Bu) ppm; HR-MS: (ESI$^+$) *m/z* $[M+H]^+$ calcd. for $C_{21}H_{36}O_2N_2$: 349.2850, found: 349.2846; IR (ATR, cm^{-1}) $\tilde{\upsilon}$: 1674 (s), 1542 (m), 1439 (m), 1360 (m), 1228 (m), 578 (w);

2.7. Synthesis of 2-((3,5-di-tert-butyl-2-hydroxybenzyl)amino)-N-phenylacetamide (HL3)

For the synthesis of **HL3**, 1 equiv. of 2-amino-*N*-phenylacetamide [21] (540 mg, 3.6 mmol) as well as 120 mg of Pd/C (5 wt% Pd) were added to a solution of 1 equiv. of 3,5-di-*tert*-butyl-2-hydroxybenzaldehyde (842 mg, 3.6 mmol) in 50 mL of MeOH. The resulting yellowish clouded solution was subsequently stirred at 50 °C in a pressure reactor under H_2 atmosphere (5 atm) for 24 h. The reaction solution was subsequently filtered and the brownish filtrate evaporated *in vacuo*. The crude beige solid was purified via column chromatography on silica gel (ethyl acetate/cyclohexane gradient from 20% to 100% ethyl acetate) to give **HL3** as white solid (601 mg, 45%). ^{1}H NMR (300 MHz, $(CD_3)_2SO$, 25 °C, amine NH obscured) δ: 11.43 (bs, 1H, OH), 10.00 (bs, 1H, NH), 7.61 ("d", 2H, ArH), 7.31 ("t", 2H, ArH), 7.10 (d, 1H, ArH), 7.05 ("t", 1H, ArH), 6.89 (d, 1H, ArH), 3.88 (s, 2H, CH_2), 3.41 (s, 2H, CH_2), 1.37 (s, 9H, *t*Bu), 1.23 (s, 9H, *t*Bu) ppm; ^{13}C NMR (75 MHz, $(CD_3)_2SO$, 25 °C) δ: 169.06 (C=O), 154.28 (Ar-O), 139.47, 138.88, 134.56, 128.77 (2x), 123.33, 123.25, 122.42, 121.77, 119.05 (2x) (Ar), 51.97, 50.40 (CH_2), 34.45, 33.77 (q-*t*Bu), 31.56, 29.55 (*t*Bu) ppm; HR-MS: (ESI$^+$) *m/z* $[M+H]^+$ calcd. for $C_{23}H_{32}O_2N_2$: 369.2537, found: 369.2534; IR (ATR, cm^{-1}) $\tilde{\upsilon}$: 1665 (m), 1518 (s), 1481 (m), 1437 (s), 1234 (m), 1103 (w), 879 (w), 761 (s), 694 (s), 537 (w), 500 (m);

2.8. Synthesis of N-(tert-butyl)-2-((3,5-dichloro-2-hydroxybenzyl)amino)acetamide (HL4)

For the synthesis of **HL4**, 1 equiv. of 2-amino-*N*-(*tert*-butyl)acetamide [21] (687 mg, 5.2 mmol) as well as 1 equiv. of 3,5-dichloro-2-hydroxybenzaldehyde (1000 mg, 5.2 mmol) in 5 mL of MeOH. The initially deep yellow solution was subsequently stirred at 50 °C for 4 h, whereupon a dark yellow precipitate started to form. The precipitate was subsequently filtered off, washed with 2 × 5 mL of pentane and dried in vacuo. The resulting orange solid was subsequently dissolved in 10 mL of MeOH and 4 equiv. of $NaBH_4$ (787 mg, 20.8 mmol) were added portionwise, accompanied by gas evolution and decoloration of the reaction solution. Subsequently the clear reaction solution was stirred overnight at room temperature. After evaporation *in vacuo*, the crude oily substance was purified via column chromatography on silica gel (ethyl acetate/cyclohexane gradient from 20% to 100% ethyl acetate) to give **HL4** as pale pink solid (600 mg, 38%). ^{1}H NMR (300 MHz, $(CD_3)_2SO$, 25 °C) δ: 7.85 (bs, 2H, NH_2^+), 7.55 (bs, 1H, NH), 7.34 (d, 1H, ArH), 7.10 (d, 1H, ArH), 3.81 (s, 2H, CH_2), 3.10 (s, 2H, CH_2), 1.26 (s, 9H, *t*Bu) ppm; ^{13}C NMR (75 MHz, $(CD_3)_2SO$, 25 °C) δ: 169.10 (C=O), 153.00 (Ar-O), 127.35, 127.07, 127.02, 121.43, 120.55 (Ar), 50.14, 50.06 (CH_2), 50.04 (q-*t*Bu), 28.49 (*t*Bu) ppm; HR-MS: (ESI$^+$) *m/z* $[M+H]^+$ calcd. for $C_{13}H_{18}O_2N_2Cl_2$: 305.0818, found: 305.0815; IR (ATR, cm^{-1}) $\tilde{\upsilon}$: 1646 (s), 1574 (m), 1451 (s), 1297(s), 1217 (s), 1166 (m), 886 (m), 735 (s), 458 (m);

2.9. Complex syntheses

All dinuclear complexes are stable towards air and moisture in solid state and can be stored at ambient conditions for several weeks without decomposition. Mononuclear complexes are stable towards air but slightly sensitive towards moisture. They can be stored in a desiccator over P_2O_5 for several weeks without decomposition.

2.10. Synthesis of [{MoO_2(L1)}$_2$(μ-O)] (1)

For the synthesis of **1**, 1 equiv. of $[MoO_2(acac)_2]$ (111 mg, 0.34 mmol) was added to a solution of 1 equiv. of **HL1** (80 mg, 0.34 mmol) in 5 mL of MeCN. The orange reaction mixture was stirred for 2 h at 60 °C whereupon the formed dark yellow precipitate was filtered off and washed with a small amount of cold MeCN and twice with 5 mL of pentane. Evaporation of all volatiles *in vacuo* led to 1 as dark yellow powder (90%, 113 mg). Crystals suitable for single–crystal X–ray diffraction analysis were obtained via recrystallization from a concentrated MeCN solution at 5 °C. ^{1}H NMR (300 MHz, $(CD_3)_2SO$, 25 °C, major isomer) δ: 8.40 (s, 2H, CONH), 7.10-7.02 (m, 4H, ArH), 6.67-6.62 (m, 2H, ArH), 6.54-6.52 (m, 2H, ArH), 5.50 (d, 2H, NH), 4.18-4.14 (m, 2H, CH_2), 4.00-3.87 (m, 2H, CH_2), 3.60-3.56 (m, 2H, CH_2), 3.14-3.08 (m, 2H, CH_2), 1.00 (s, 18H, *t*Bu) ppm; ^{1}H NMR (300 MHz, $(CD_3)_2SO$, 25 °C, minor isomer) δ: 8.40 (s, 2H, CONH), 7.10-7.02 (m, 4H, ArH), 6.67-6.62 (m, 2H, ArH), 6.54-6.52 (m, 2H, ArH), 5.18 (d, 2H, NH), 4.18-4.14 (m, 2H, CH_2), 4.00-3.87 (m, 2H, CH_2), 3.60-3.56 (m, 2H, CH_2), 3.14-3.08 (m, 2H, CH_2), 1.02 (s, 18H, *t*Bu) ppm; ^{13}C NMR (75 MHz, $(CD_3)_2SO$, 25 °C, major isomer) δ: 173.33 (C=O), 162.79 (Ar-O), 129.93, 129.29, 123.42, 119.20, 118.31 (Ar), 51.73 (CH_2), 51.67 (q-*t*Bu), 27.95 (*t*Bu) ppm; IR (ATR, cm^{-1}) $\tilde{\upsilon}$: 1624 (m), 1480 (w), 1262 (m), 930 (m), 899 (s), 878 (s), 753 (s, br), 726 (s), 617 (s), 496 (m), 478 (m), 388 (w); HR-MS: (ESI$^+$) *m/z* $[M+H]^+$ calcd. for $C_{26}H_{38}O_9N_4Mo_2$: C, 743.0829, found: 743.0829; Anal. calcd. for $C_{26}H_{38}Mo_2N_4O_9$: C, 42.06; H, 5.16; N, 7.55. Found: C, 42.50, H, 5.08; N, 7.37%.

2.11. Synthesis of [MoO_2(L1)(OMe)] (2)

For the synthesis of **2**, 1 equiv. of $[MoO_2(acac)_2]$ (200 mg, 0.61 mmol) was added to a solution of 1 equiv. of **HL1** (142 mg, 0.61 mmol) in 5 mL of MeOH. The yellowish reaction mixture was stirred for 4 h at 50 °C whereupon the formed pale yellow precipitate was filtered off and washed twice with a small amount of cold MeOH. Evaporation of all volatiles *in vacuo* led to 2 as pale yellow powder (86%, 246 mg). Crystals suitable for single–crystal X–ray diffraction analysis were obtained via recrystallization from a concentrated MeOH solution at 5 °C. ^{1}H NMR (300 MHz, $(CD_3)_2SO$, 25 °C) δ: 8.57 (s, 1H, CONH), 7.12-7.05 (m, 2H, ArH), 6.69-6.64 (m, 1H, ArH), 6.57-6.55 (m, 1H, ArH), 5.92 (d, 1H, NH), 4.20-4.15 (m, 1H, CH_2), 4.01 (s, 3H, OMe), 3.51-3.42 (m, 2H, CH_2), 3.18-3.12 (m, 1H, CH_2), 1.00 (s, 9H, *t*Bu); ^{13}C NMR (75 MHz, $(CD_3)_2SO$, 25 °C) δ: 173.26 (C=O), 162.33 (Ar-O), 130.02, 129.42, 119.16, 118.50 (Ar), 64.36 (OMe), 52.15 (CH_2), 51.86 (q- *t*Bu), 51.13 (CH_2), 27.76 (*t*Bu); IR (ATR, cm^{-1}) $\tilde{\upsilon}$: 1615 (s), 1574 (m), 1485 (m), 1450 (m), 1267 (m), 1050 (m), 927 (s), 878 (s), 769 (s), 620 (s), 550 (s), 500 (m), 475 (s); HR-MS: (ESI$^+$) *m/z* $[M-OMe]^+$ calcd. for $C_{14}H_{22}MoN_2O_5$: 365.0394, found: 365.0391; Anal. calcd. for $C_{14}H_{22}MoN_2O_5$: C, 42.65; H, 5.62; N, 7.10. Found: C, 42.55, H, 5.46; N, 6.93%.

2.12. Synthesis of [{MoO_2(L2)}$_2$(μ-O)] (3)

For the synthesis of **3**, 1 equiv. of [$MoO_2(acac)_2$] (100 mg, 0.31 mmol) was added to a solution of 1 equiv. of **HL2** (107 mg, 0.31 mmol) in 3 mL of MeCN. The orange reaction mixture was stirred for 6 h at 60 °C whereupon the formed orange precipitate was filtered off and washed thrice with 5 mL of pentane. Evaporation of all volatiles *in vacuo* led to **3** as an orange solid (90%, 135 mg). Crystals suitable for single–crystal X–ray diffraction analysis were obtained via slow evaporation of a concentrated $(CD_3)_2SO$ solution at room temperature. ^{1}H NMR (300 MHz, $(CD_3)_2SO$, 25 °C, major isomer) δ: 8.23 (s, 2H, CONH), 7.06 (d, 2H, ArH), 6.91 (d, 2H, ArH), 5.55 (d, 2H, NH), 4.11-3.93 (m, 4H, CH_2), 3.51-3.47 (m, 2H, CH_2), 3.20-3.10 (m, 2H, CH_2), 1.28 (s, 18H, *t*Bu), 1.23 (s, 18H, *t*Bu), 0.95 (s, 18H, *t*Bu) ppm; ^{1}H NMR (300 MHz, $(CD_3)_2SO$, 25 °C, minor isomer) δ: 8.29 (s, 2H, CONH), 7.07 (d, 2H, ArH), 6.89 (d, 2H, ArH), 5.09 (d, 2H, NH), 4.11-3.93 (m, 4H, CH_2), 3.51-3.47 (m, 2H, CH_2), 3.20-3.10 (m, 2H, CH_2), 1.30 (s, 18H, *t*Bu), 1.23 (s, 18H, *t*Bu), 0.96 (s, 18H, *t*Bu) ppm; ^{13}C NMR (75 MHz, $(CD_3)_2SO$, 25 °C, major isomer) δ: 173.38 (C=O), 159.46 (Ar-O), 139.43, 136.93, 124.60, 122.86, 122.28 (Ar), 52.79, 51.51 (CH_2), 51.41, 34.32, 33.78 (q-*t*Bu), 31.64, 29.78, 28.17 (*t*Bu) ppm; IR (ATR, cm^{-1}) $\tilde{\upsilon}$: 1621 (m), 1440 (w), 1266 (w), 910 (m), 872 (s), 853 (s), 738 (vs, br), 554 (m), 482 (w); HR-MS: (ESI$^+$) *m*/*z* [M+H]$^+$ calcd. for $C_{42}H_{70}Mo_2N_4O_9$: 968.3343, found: 968.3335; Anal. calcd. for $C_{42}H_{70}Mo_2N_4O_9$: C, 52.17; H, 7.30; N, 5.79. Found: C, 52.10, H, 6.82; N, 5.77%.

2.13. Synthesis of [MoO_2(L2)(OMe)] (4)

For the synthesis of **4**, 1 equiv. of [$MoO_2(acac)_2$] (100 mg, 0.31 mmol) was added to a solution of 1 equiv. of **HL2** (107 mg, 0.31 mmol) in 3 mL of MeOH. The yellowish reaction mixture was stirred for 6 h at 50 °C whereupon the formed yellow precipitate was filtered off and washed twice with a small amount of cold MeOH. Evaporation of all volatiles *in vacuo* led to **4** as a bright yellow solid (75%, 117 mg). Crystals suitable for single–crystal X–ray diffraction analysis were obtained via crystallization from a concentrated MeOH solution at 5 °C. ^{1}H NMR (300 MHz, $(CD_3)_2SO$, 25 °C) δ: 8.48 (s, 1H, CONH), 7.08 (d, 1H, ArH), 6.93 (d, 1H, ArH), 5.92 (d, 1H, NH), 4.13-4.09 (m, 1H, CH_2), 3.97 (s, 3H, OMe), 3.46-3.38 (m, 2H, CH_2), 3.21-3.16 (m, 1H, CH_2), 1.29 (s, 9H, *t*Bu), 1.23 (s, 9H, *t*Bu), 0.94 (s, 9H, *t*Bu); ^{13}C NMR (75 MHz, $(CD_3)_2SO$, 25 °C) δ: 173.19 (C=O), 158.90 (Ar-O), 139.79, 136.92, 124.69, 122.98, 122.39 (Ar), 65.88 (OMe), 52.85 (CH_2), 51.69 (q-*t*Bu), 51.45 (CH_2), 34.30, 33.81 (q-*t*Bu), 31.62, 29.78, 27.85 (*t*Bu); IR (ATR, cm^{-1}) $\tilde{\upsilon}$: 1622 (s), 1471 (w), 1260 (m), 1060 (m), 1032 (m), 906 (s), 888 (s), 846 (s), 600 (m), 567 (m), 520 (s), 484 (s); HR-MS: (ESI$^+$) *m*/*z* [M-OMe]$^+$ calcd. for $C_{22}H_{38}MoN_2O_5$: 477.1645, found: 477.1644; Anal. calcd. for $C_{22}H_{38}MoN_2O_5$: C, 52.17; H, 7.56; N, 5.53. Found: C, 52.10, H, 7.44; N, 5.57%.

2.14. Synthesis of [{MoO_2(L3)}$_2$(μ-O)] (5)

For the synthesis of **5**, 1 equiv. of [$MoO_2(acac)_2$] (177 mg, 0.54 mmol) was added to a solution of 1 equiv. of **HL3** (200 mg, 0.54 mmol) in 5 mL of MeCN. The orange reaction mixture was stirred for 6 h at 60 °C whereupon the formed orange precipitate was filtered off and washed thoroughly with CH_2Cl_2. Evaporation of all volatiles *in vacuo* led to **5** as an orange solid (96%, 260 mg). Crystals suitable for single–crystal X–ray diffraction analysis were obtained via slow evaporation of a concentrated MeCN solution at room temperature. IR (ATR, cm^{-1}) $\tilde{\upsilon}$: 1628 (w), 1569 (w), 1452 (w), 1264 (w), 1072 (w), 921 (m), 887 (s), 853 (m), 778 (s), 752 (s), 553 (m), 491 (w); HR-MS: (ESI$^+$) *m*/*z* [M+H]$^+$ calcd. for $C_{46}H_{62}Mo_2N_4O_9$: 1008.2719, found: 1008.2713; Anal. calcd. for $C_{46}H_{62}Mo_2N_4O_9{\cdot}0.5CH_2Cl_2$: C, 53.22; H, 6.05; N, 5.34. Found: C, 53.11, H, 6.01; N, 5.51%.

2.15. Synthesis of [MoO_2(L3)(OMe)] (6)

For the synthesis of **6**, 1 equiv. of [$MoO_2(acac)_2$] (100 mg, 0.31 mmol) was added to a solution of 1 equiv. of **HL3** (89 mg, 0.31 mmol) in 5 mL of MeOH. The yellowish reaction mixture was stirred for 6 h at 50 °C whereupon the formed yellow precipitate was filtered off and washed twice with a small amount of cold MeOH. Evaporation of all volatiles *in vacuo* led to **6** as a bright yellow solid (82%, 116 mg). Crystals suitable for single–crystal X–ray diffraction analysis were obtained via recrystallization from a concentrated MeOH solution at 5 °C. ^{1}H NMR (300 MHz, $(CD_3)_2SO$, 25 °C) δ: 10.65 (s, 1H, CONH), 7.26-7.21 (m, 2H, ArH), 7.14-7.10 (m, 1H, ArH), 7.04-6.97 (m, 4H, ArH), 6.09 (d, 1H, NH), 4.21-4.17 (m, 1H, CH_2), 4.03 (s, 3H, OMe), 3.79-3.71 (m, 1H, CH_2), 3.57-3.53 (m, 1H, CH_2), 3.37-3.31 (m, 1H, CH_2), 1.23 (s, 9H, *t*Bu), 1.12 (s, 9H, *t*Bu); ^{13}C NMR (75 MHz, $(CD_3)_2SO$, 25 °C) δ: 173.17 (C=O), 158.69 (Ar-O), 140.37, 137.30, 135.77, 128.41 (2x), 125.61, 124.86, 123.24, 122.43, 121.79 (2x) (Ar), 66.58 (OMe), 52.74, 51.56 (CH_2), 34.30, 33.76 (q-*t*Bu), 31.41, 29.69 (*t*Bu); IR (ATR, cm^{-1}) $\tilde{\upsilon}$: 1627 (m), 1593 (w), 1568 (w), 1062 (w), 923 (m), 884 (s), 845 (s), 753 (m), 598 (m), 506 (s); HR-MS: (ESI$^+$) *m*/*z* [M-OMe]$^+$ calcd. for $C_{24}H_{34}MoN_2O_5$: 497.1332, found: 497.1337, [M+H]$^+$ calcd. for $C_{24}H_{34}MoN_2O_5$: 529.1600, found: 529.1597; Anal. calcd. for $C_{24}H_{34}MoN_2O_5$: C, 54.75; H, 6.51; N, 5.32. Found: C, 54.63, H, 6.03; N, 5.43%.

2.16. Synthesis of [{MoO_2(L4)}$_2$(μ-O)] (7)

For the synthesis of **7**, 1 equiv. of [$MoO_2(acac)_2$] (107 mg, 0.33 mmol) was added to a solution of 1 equiv. of **HL4** (100 mg, 0.33 mmol) in 5 mL of MeCN. The yellow reaction mixture was stirred for 4 h at 60 °C whereupon the formed bright yellow precipitate was filtered off and dried *in vacuo* to give **7** as a pale yellow solid (82%, 119 mg). ^{1}H NMR (300 MHz, $(CD_3)_2SO$, 25 °C, major isomer) δ: 8.63 (s, 2H, CONH), 7.31 (d, 2H, ArH), 7.18 (d, 2H, ArH), 5.76 (d, 2H, NH), 4.10-4.01 (m, 2H, CH_2), 3.92-3.77 (m, 2H, CH_2), 3.71-3.67 (m, 2H, CH_2), 3.19-3.13 (m, 2H, CH_2), 1.07 (s, 18H, *t*Bu) ppm; ^{1}H NMR (300 MHz, $(CD_3)_2SO$, 25 °C, minor isomer) δ: 8.56 (s, 2H, CONH), 7.30 (d, 2H, ArH), 7.16 (d, 2H, ArH), 5.53 (d, 2H, NH),), 4.10-4.01 (m, 2H, CH_2), 3.92-3.77 (m, 2H, CH_2), 3.63-3.59 (m, 2H, CH_2), 3.19-3.13 (m, 2H, CH_2), 1.05 (s, 18H, *t*Bu) ppm; ^{13}C NMR (75 MHz, $(CD_3)_2SO$, 25 °C, major isomer) δ: 173.62 (C=O), 157.81 (Ar-O), 128.49, 128.36, 124.57, 120.89 (Ar), 52.79, 52.03 (q-*t*Bu), 51.00 (2 x CH_2), 27.81 (*t*Bu) ppm; IR (ATR, cm^{-1}) $\tilde{\upsilon}$: 1622 (s), 1458 (m), 922 (s), 899 (s), 785 (s), 750 (vs, br), 563 (w), 478 (w); HR-MS: (ESI$^+$) *m*/*z* [M+H]$^+$ calcd. for $C_{26}H_{34}Cl_4Mo_2N_4O_9$: 882.9238, found: 882.9232; Anal. calcd. for $C_{26}H_{34}Cl_4Mo_2N_4O_9$: C, 35.48; H, 3.89; N, 6.36. Found: C, 35.29, H, 3.90; N, 6.15%.

3. Results and discussion

3.1. Ligand synthesis

Ligands **HL1**–**HL3** were prepared according to Scheme 1. Thus, the respective hydroxybenzaldehydes were reacted with functionalized amidoamines under H_2 atmosphere (5 atm) in a pressure reactor over Pd/C. The products were obtained in fair yields after purification via column chromatography.

Ligand **HL4** was prepared in a two-step procedure according to Scheme 2. In the first step, 2-hydroxy-3,5 dichlorobenzaldehyde was condensed with the respective amine. The formed Schiff base was subsequently treated with an excess of sodium borohydride. Column chromatography gave the desired product in fair yield. A

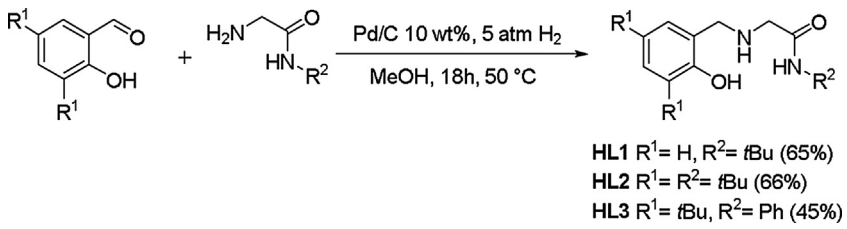

Scheme 1. Synthesis of the aminophenolate amide ligands **HL1–HL3**.

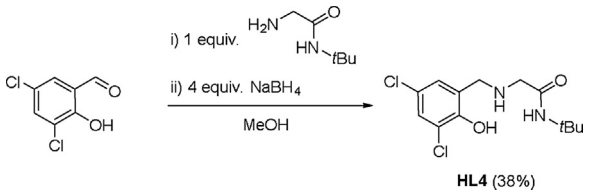

Scheme 2. Synthesis of the aminophenolate amide ligand **HL4**.

synthesis procedure using H_2 and Pd/C did not yield an isolable amount of **HL4**.

The employed functionalized primary amines were prepared according to published procedures [21]. Ligands **HL1**–**HL4** were characterized via ^{1}H, ^{13}C NMR, FT-IR and HR-MS (ESI$^+$) spectroscopy. Noteworthy is the difference in the shift of the amide NH proton, depending on the substituent (7.53 ppm in **HL2** and 10.00 ppm in **HL3**, *tert*–butyl vs. phenyl amide, $(CD_3)_2SO$). Another interesting feature arises from a comparison of the ^{1}H NMR spectra of **HL1-HL4** in $(CD_3)_2SO$. Whereas the OH and NH protons are not observable in ligands **HL1** and **HL2**, likely due to fast exchange, they are clearly assignable for ligand **HL3**. For the dichloro-substituted ligand **HL4** on the other hand ^{1}H NMR spectroscopy in $(CD_3)_2SO$ displays resonances which are assignable to an O^-- NH_2^+ form, suggesting a zwitterionic behavior in solution (Fig. S1). Ligands **HL1**-**HL4** feature electron withdrawing and donating substituents at the phenolate and amide moieties, respectively, allowing for an assessment of electronic influences on the properties of the resulting molybdenum complexes.

3.2. Complex synthesis

The synthesis of the dinuclear complexes **1**, **3**, **5** and **7** of the type $[\{MoO_2\mathbf{L}\}_2(\mu\text{-}O)]$ was accomplished via the reaction of one equiv. of **HL1**-**HL4**, respectively, with one equiv. of $[MoO_2(acac)_2]$ in MeCN under ambient conditions in excellent yields (Scheme 3).

The bridging oxygen atom likely originates from the deprotonation of advantageous water molecules, possibly via a hydroxido intermediate, as previously disclosed for related complexes [18]. This assumption is corroborated by the formation of only traces of complex **3**, accompanied by insoluble solids, if the synthesis is carried out under inert conditions in dry MeCN. Interestingly, if the protic solvent MeOH is employed in the synthesis, complexes **2**, **4** and **6** of the general formula $[MoO_2\mathbf{L}(OMe)]$ were obtained in good to excellent yield both under ambient and inert conditions (Scheme 3). The formation of this mononuclear complexes marks an interesting contrast to previous observations, where the use of standard grade methanol also led to dinuclear compounds [18]. We attribute the formation of the mononuclear complexes to the similar acidity of the protons in H_2O and MeOH and the vast excess of the latter in MeOH solution [26]. If less acidic alcoholic solvents are employed (e.g. *i*PrOH, *t*BuOH), no formation of the respective alcoholate complexes could be observed. The higher steric demand of an isopropyl or *tert*-butyl group could also inhibit the formation of such complexes.

Complexes **1**–**7** feature one ligand moiety per molybdenum center, coordinated in a facial ONO motif via the anionic phenolate, the amine and the carbonyl oxygen of the amide, as observed in the solid state structures of **1**–**3**, **5** and **6**. The ^{1}H NMR spectra of the methanolate complexes **2**, **4** and **6** feature the expected one set of shifted ligand resonances, including a broadened doublet for the proton at the coordinated amine. Interestingly, in the spectra of the dinuclear μ-oxido complexes two sets of ligand resonances with a solvent dependent ratio (e.g. 3:2 in $(CD_3)_2CO$ and 5:2 in $(CD_3)_2SO$ for complex **3**, Fig. S4) were observed. Dissolving single crystals of **3** and immediate ^{1}H NMR measurement resulted in analogous spectra, hinting towards a dynamic isomerization in solution. Considering free rotation around the μ-oxido Mo-O bonds, X-ray data suggests two homotopic half units (*vide infra*), which would result in only one signal set observable by NMR spectroscopy. If the two halves would be non-homotopic, two signal sets in a ratio of 1:1 should result. To gain further insight, we performed VT-NMR measurements in $(CD_3)_2SO$ (20 °C to 60 °C) as well as in CD_3CN (−30 °C to 60 °C, Fig. S2) which unfortunately did not show any meaningful change in the ratio of the signal sets and thus do not allow for clear assertion of the dynamics in solution. However, it is possible that the observed resonances arise from a labile coordination of the amide moieties, resulting in an equilibrium between five- and a sixfold coordinated metal centers.

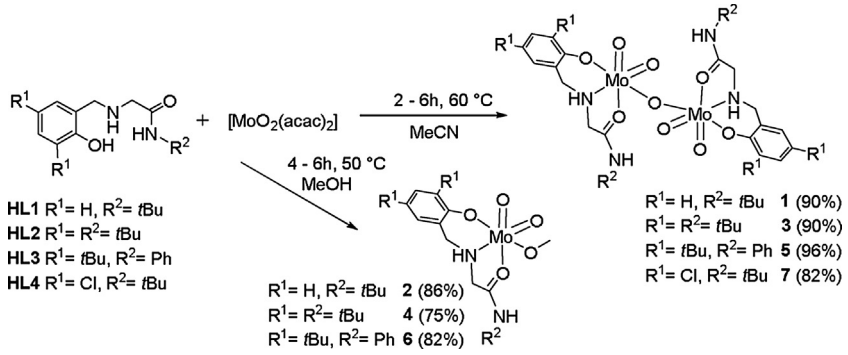

Scheme 3. Synthesis of complexes **1**–**7**.

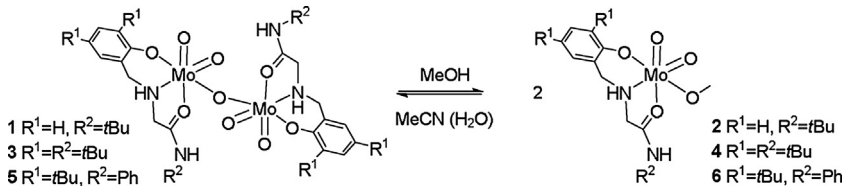

Scheme 4. Interconversion of mononuclear and dinuclear molybdenum complexes.

Table 1
Selected crystallographic data and structure refinement for complexes **1**–**3, 5** and **6.**

	1	**2**	**3**[a]	**5**	**6**[a]
Empirical formula	$C_{26}H_{38}Mo_2N_4O_9$	$C_{14}H_{22}MoN_2O_5$	$C_{42}H_{70}Mo_2N_4O_9{\cdot}3C_2H_6OS$	$C_{46}H_{62}Mo_2N_4O_9{\cdot}3C_2H_3N$	$C_{24}H_{34}MoN_2O_5{\cdot}CH_3OH$
Formula weight	742.48	394.27	1201.28	1130.03	558.51
Crystal description	needle, yellow	needle, colorless	block, yellow	block, yellow	block, yellow
Crystal system, space group	monoclinic, C 2/c	monoclinic, P 2_1/c	orthorhombic, P 2_1 2_1 2_1	triclinic, P −1	triclinic, P −1
a [Å]	35.8689(16)	12.734(2)	11.7746(6)	10.3527(7)	9.5849(9)
b [Å]	7.3863(3)	6.8362(12)	29.8324(15)	15.5833(12)	16.7996(17)
c [Å]	27.2284(12)	18.769(4)	33.3041(17)	18.3910(13)	18.4598(18)
α [°]				73.523(3)	113.094(3)
β [°]	115.7437(13)	91.201(5)		77.913(4)	95.732(4)
γ [°]				75.891(3)	98.174(3)
Volume [Å^3]	6497.8(5)	1633.5(5)	11698.5(10)	2727.8(3)	2666.6(5)
Z	8	4	8	2	4
Reflections collected/unique	51941/9491	18825/3211	63089/22972	64481/24013	152692/23463
R(int), R(sigma)	0.0390, 0.0339	0.0493, 0.0518	0.0452, 0.0769	0.0537, 0.0604	0.0438, 0.0266
Completeness (Θ_{max})	100.0% (30.0°)	99.9% (26.0°)	99.8% (26.0°)	100.0% (35.0°)	99.9% (35.0°)
Data/parameters/restraints	9491/404/4	3211/220/2	22972/1349/74	24013/685/4	23463/677/6
Signif. unique refl. [I > 2σ(I)]	8077	2621	18476	19319	20033
Goodness-of-fit on F^2	1.040	1.144	1.114	1.037	1.047
Final R indices [I > 2σ(I)]	R1 = 0.0264, wR2 = 0.0580	R1 = 0.0402, wR2 = 0.0728	R1 = 0.0546, wR2 = 0.1420	R1 = 0.0344,wR2 = 0.0833	R1 = 0.0239, wR2 = 0.0577
R indices (all data)	R1 = 0.0353, wR2 = 0.0603	R1 = 0.0574, wR2 = 0.0824	R1 = 0.0678, wR2 = 0.1480	R1 = 0.0477,wR2 = 0.0893	R1 = 0.0332, wR2 = 0.0631
Largest difference peak and hole [e/Å^3]	0.746 and −0.516	0.845 and −0.828	1.276 and −1.098	0.890 and −1.415	0.836 and −0.667
CCDC - Number	1532978	1532979	1532980	1532981	1532982

[a] Parameters corresponding to the second observed modification are provided within the SI.

We were interested if the different complexes formed in MeCN and MeOH are able to interconvert. For this reason, the following observation is of importance. If the dinuclear complexes are dissolved in MeOH, the color of the solution brightened within minutes and removal of the solvent after 24 h of standing at room temperature yielded the respective methanolate complex in quantitative yield. A similar effect was observed upon dissolving the methanolate complexes in benchtop MeCN (Scheme 4).

To obtain insight into the behavior of the complexes under catalytic conditions *(vide infra)*, a mixture of complex **3** and ten equiv. of TBHP was dissolved in benchtop CD_3CN (the solubility in $CDCl_3$ was not sufficient to obtain meaningful spectra) and stirred for 24 h at 50 °C. A ^{1}H NMR spectrum of the reaction solution recorded after 24 h showed no observable difference to the spectrum of the initial complex (Fig. S3), revealing a surprisingly high stability under these conditions. The NMR measurement repeated after leaving the sample for 30 days under ambient conditions and also after subsequent addition of ~500 equiv. of H_2O still showed no substantial decomposition, again in contrast to other published precatalysts [9,12,17].

3.3. Molecular structures

Molecular structures of dinuclear complexes **1, 3** and **5**, as well as mononuclear complexes **2** and **6** were determined by single–crystal X–ray diffraction analysis. For complex **3**, racemic twinning was observed, and for **6** two independent molecules (labelled **A** and **B**, only molecule **A** discussed here, for **B** please refer to the SI) with distinct structural differences were found in the solid state. Molecular views of **1, 3** and **5** are given in Fig. 1, and of **2** and **6** in Fig. 2. Selected crystallographic data for complexes **1-3** and **5–6** are provided in Table 1, selected bond lengths and angles are given in Table 2, full crystallographic details such as intra- and intermolecular hydrogen bonding, structure refinement and experimental details are provided within the SI.

In the μ-oxido bridged dinuclear complexes **1**, **3** and **5** each molybdenum center is coordinated in a distorted octahedral fashion by two oxido ligands, one facially ONO-coordinating tridentate ligand as well as the bridging oxygen atom. General features of these complexes are the rather long distances between the molybdenum atoms and the bonding amino and carbonyl groups, respectively (Table 2). Despite the similarity of these complexes, clear differences can be observed with respect to the Mo1–O1–Mo2 angle, i.e. the linearity of the μ-oxido bridge, as well as the dihedral angles between the oxido groups on Mo1 and Mo2 (e.g. O2–Mo1–Mo2–O4). Whereas the Mo1–O1–Mo2 angles in **1** and **3** exhibit smaller deviations from 180° (166.94(7)° in **1** and 175.2(4)/170.1(3)° in **3**), the Mo1–O1–Mo2 angle observed for complex **5** is 146.96(5)°. Both, linear (Mo-O-Mo angle close to 180°) and bent structures (Mo-O-Mo angle <180°) have been observed in previously reported dinuclear dioxidomolybdenum(VI) complexes [18]. Also, whereas the dihedral O-Mo-Mo-O angles in complexes

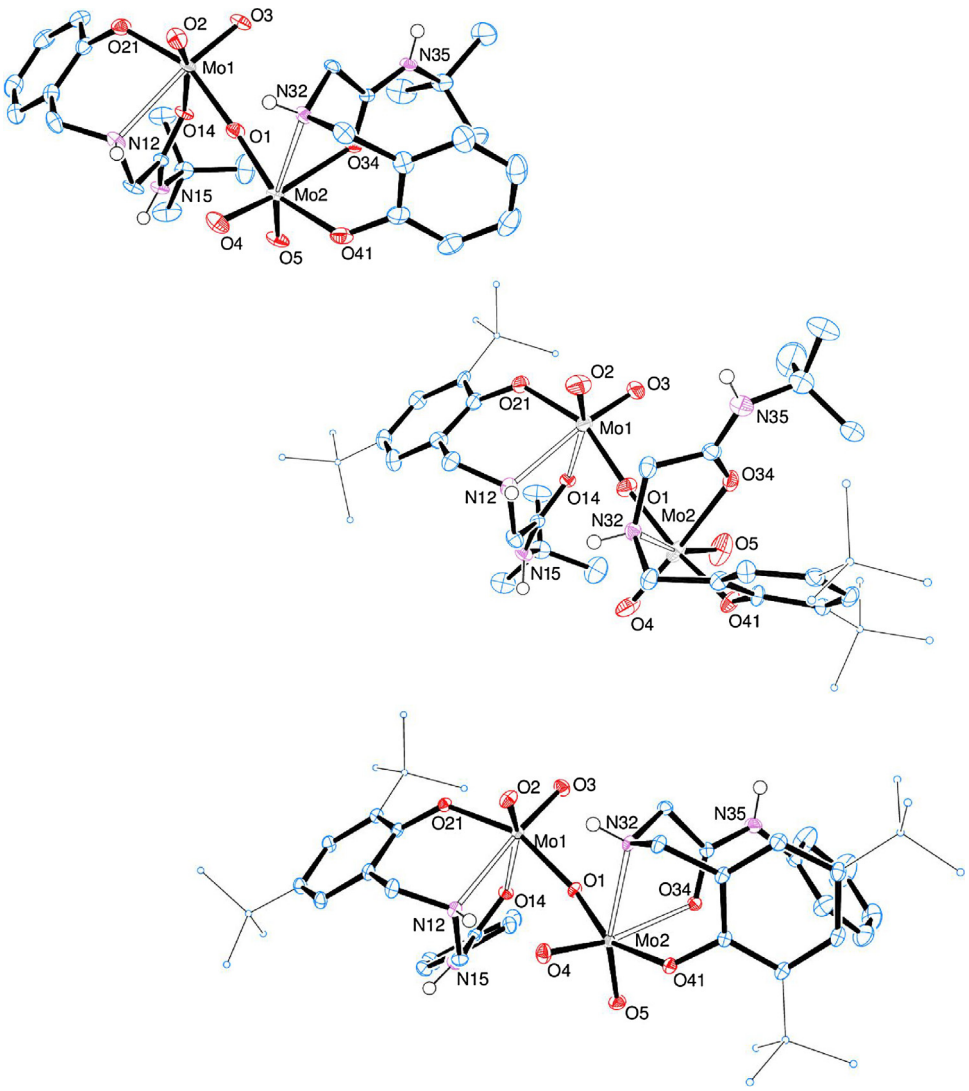

Fig. 1. Molecular views (50% probability level) of **1** (top), **3** (middle) and **5** (bottom); H atoms (except nitrogen bound protons) as well as solvent molecules are omitted for clarity reasons. Open bonds depict unusual long Mo–L contacts. The tert–butyl substituents on the phenyl rings in **3** and **5** are drawn with small spherical atoms and line bonds for clarity reasons.

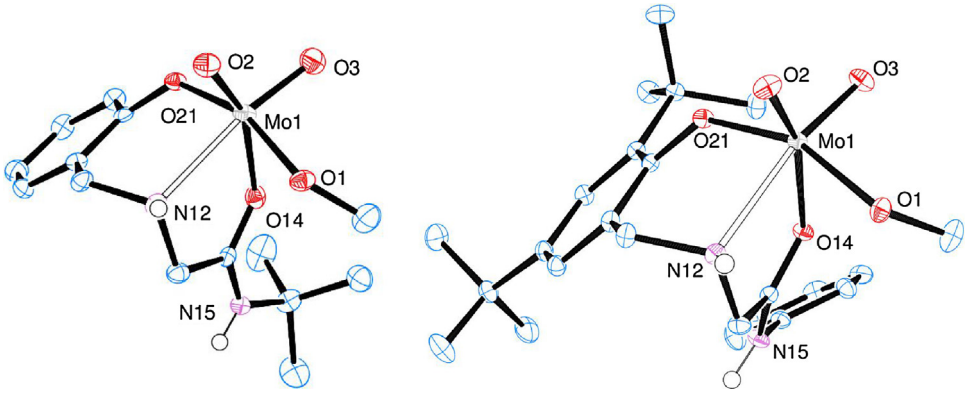

Fig. 2. Molecular views (50% probability level) of **2** (left), and **6** (right); H atoms (except nitrogen bound protons) as well as solvent molecules are omitted for clarity reasons. Open bonds depict unusual long Mo–L contacts.

1 and **5** are comparable (300° and 302°), the complex half units in **3** are rotated around the μ-oxido bridge (243°), further corroborating the geometric flexibility of the complexes (Table 2).

In the mononuclear complexes **2** and **6**, the molybdenum center is coordinated in a distorted octahedral fashion that closely resembles the coordination environment of the related dinuclear

Table 2
Selected bond lengths [Å] and angles [°] for complexes **1**–**3**, **5** and **6**.

	1	2	3[a]	5	6[a]
Mo1—O1	1.8994(12)	1.923(2)	1.885(5)	1.9049(9)	1.9237(8)
Mo1—O2	1.7149(12)	1.710(3)	1.707(6)	1.7245(9)	1.7172(8)
Mo1—O3	1.7202(11)	1.728(3)	1.715(5)	1.7122(10)	1.7221(8)
Mo1—O21	1.9555(12)	2.002(2)	1.979(5)	1.9791(9)	1.9520(7)
Mo1—O14	2.2231(11)	2.227(3)	2.307(5)	2.2613(9)	2.2257(7)
Mo1—N12	2.3952(13)	2.361(3)	2.355(5)	2.3623(11)	2.3617(9)
Mo2—O1	1.8795(12)	–	1.919(5)	1.9141(9)	–
Mo2—O4	1.7131(12)	–	1.723(6)	1.7178(10)	1.7137(8)
Mo2—O5	1.7180(12)	–	1.721(5)	1.7129(10)	1.7245(8)
Mo2—O6	–	–	–	–	1.9333(8)
Mo2—O41	1.9797(13)	–	1.987(5)	1.9807(9)	1.9570(7)
Mo2—O34	2.2222(11)	–	2.245(5)	2.2929(9)	2.2833(7)
Mo2—N32	2.3915(13)	–	2.390(4)	2.3650(11)	2.3378(8)
Mo1—O1—Mo2	166.94(7)	–	175.2(4)	146.96(5)	–
O2—Mo1—O3	105.20(6)	107.11(13)	105.6(3)	105.97(5)	107.11(4)
O4—Mo2—O5	105.19(6)	–	105.7(3)	106.79(5)	107.89(4)
O2—Mo1—Mo2—O4	300.94(6)	–	243.03(27)	302.10(5)	–
O2—Mo1—Mo2—O5	194.55(7)	–	135.46(27)	196.51(5)	–

[a] Only data for one molecule shown, bond lengths and angles for other molecule shown in SI.

Table 3
Overview of conversion of substrate (selectivity to epoxide) with TBHP as oxidant.

	1	2	3	4	5	6	7
S1	59 (92)	41 (89)	>95 (>95)[a]	68 (>95)	75 (91)	79 (>95)	>95 (>95)[b]
S2	no conv.	no conv.	33 (70)	no conv.	no conv.	no conv.	32 (92)
S3	unsel.	61 (8)	69 (22)	unsel.	unsel.	83 (34)	27 (30)
S4	61 (34)	60 (11)	65 (69)	51 (42)	87 (43)	>95 (49)	66 (69)
S5	60 (10)	no conv.	>95 (86)	81 (31)	85 (22)	no conv.	56 (58)

General conditions: 2 equiv. TBHP (5.5 M in decane), 50 °C, $CHCl_3$, 0.001 mol% precatalyst loading; conversion of substrate (%) after 24 h, as determined by GC–MS (selectivity in % for epoxide in brackets); no conv. = substrate was not converted; unsel.= substrate was converted, but epoxide was not formed or consumed over reaction time.
[a] After 8 h reaction time.
[b] After 4 h reaction time.

compounds **1** and **5**. Instead of the μ-oxido bridge, the sixth coordination site in complexes **2** and **6** is occupied by a monoanionic methoxide ligand. Most bond lengths are similar to the respective dinuclear complexes with the exception of the Mo1–O1 bond to the methoxido ligand which is longer than to the μ-oxido bridging atom. In general, the observed molybdenum oxido bond lengths are within expected ranges for all reported complexes (Table 2) [27]. For all structurally characterized complexes, inter- and intra-molecular hydrogen bonding is observed (Tables S4, S7, S10, S13, S16 and S19). For dinuclear complexes **1**, **3** and **5** intramolecular hydrogen bonding is especially pronounced in **5**, and less pronounced in **1** and **3**. In these complexes, hydrogen bonds are spanning the two halves of the molecule across the μ-oxido bridging atom, between the amine N-*H* atom and a terminal oxido ligand (Fig. S12). In addition, all three complexes **1**, **3** and **5** show inter-molecular hydrogen bonding to neighboring complexes in the solid state. For mononuclear complexes **2** and **6**, hydrogen bonds between the amide N-*H* atom and the methoxide oxygen atom are observed, validating the ability of ligands **HL1-4** to provide hydrogen bonding.

3.4. Olefin epoxidation

Complexes **1-7** were screened in the catalytic epoxidation of various internal and terminal olefins using two equiv. of *tert*-butylhydroperoxide (TBHP, 5.5 M in decane) or hydrogen peroxide (H_2O_2, 30% in water) as oxygen source (Fig. 3). All catalyst loadings as well as TONs are calculated per complex molecule (*vide infra*). Blank reactions without added catalysts were performed for all substrates and showed conversions below 10% (uncatalyzed reactions).

In an initial round, the five substrates **S1-S5** were tested under previously optimized reaction conditions (50 °C, 2 equiv. oxidant, $CHCl_3$).

Table 4
Overview of conversion of substrate (selectivity to epoxide) with H_2O_2 as oxidant.

	1	3	4	5
S1	32 (>95)	74 (87)	89 (95)	87 (93)
S2	no conv.	30 (77)	no conv.	28 (93)
S3	no conv.	no conv.	no conv.	no conv.
S4	no conv.	64 (27)	39 (31)	65 (10)
S5	no conv.	unsel.	no conv.	unsel.

General conditions: 2 equiv. H_2O_2 (30 wt% in water), 50 °C, $CHCl_3$, 0.1 mol% precatalyst loading; conversion of substrate (%) after 24 h, as determined by GC–MS (selectivity in % for epoxide in brackets); no conv. = substrate was not converted; unsel.= substrate was converted, but no epoxide was formed or consumed over reaction time; **2, 6** and **7** were unproductive/unselective, results not shown.

With TBHP as oxidant, all complexes reached average to high substrate conversions, even at very low precatalyst loadings of 0.001 mol%, except for substrate **S2** (Table 3). For 1-octene **S2**, only complex **3** and **7** gave low conversions under these conditions. For aqueous oxidant H_2O_2, only complexes **1**, **3**, **4** and **5** gave noticeable conversions at the higher precatalyst loading of 0.1 mol% (Table 4). A comparison of turnover numbers (TON) for all seven complexes with both oxidants is given in Table 5.

In accordance to literature, also precatalysts **1-7** show higher epoxidation activity with organic oxidant TBHP compared to aqueous oxidant H_2O_2. Whilst conversion of cyclooctene **S1** and selectivity for epoxide with TBHP was high in all cases, the more challenging substrates **S2-5** showed a different picture. Only two (**3** and **7**) out of the seven complexes showed activity for 1-octene **S2**, albeit with low conversions. For styrene **S3** epoxidations suffered from un-selectivity (0–34%) due to over-oxidation of the initially formed epoxide to phenylacetaldehyde and benzaldehyde. Epoxidation of cyclic substrate limonene **S4** was selective for the endocyclic double bond, but selectivity overall (11–69%) suffered

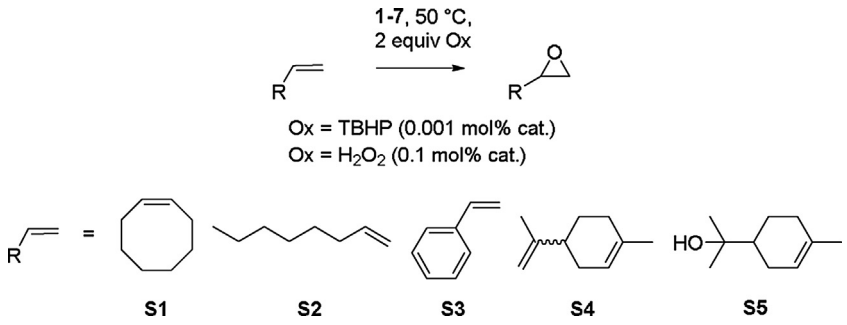

Fig. 3. Epoxidations of olefinic substrates **S1-S5** by complexes **1-7**.

Table 5
Overview of TONs for epoxidations using TBHP/H_2O_2.

	1	2	3	4	5	6	7
S1	75,500/270	36,700/0	95,300/650	66,400/830	68,400/790	77,600/0	110,000/0
S2	0/0	0/0	23,100/230	0/0	0/200	0/0	32,400/0
S3	0/0	4500/0	15,000/0	0/0	0/0	28,400/0	27,200/0
S4	46,400/0	6800/0	44,700/270	21,500/120	37,600/60	48,000/0	66,300/0
S5	29,500/0	0/0	83,500/0	25,000/0	18,600/0	0/0	56,200/0

TON is calculated per complex molecule.

from subsequent over-oxidation of the formed epoxide to the cyclohexanone carvone. An almost similar catalytic profile was observed for hydroxy containing substrate α-terpineol **S5**, with the exception of precatalyst **3**. For precatalysts **1**, **4**, **5** and **7**, selectivity for epoxide with **S5** was low (10–58%) due to over-oxidation, whereas mononuclear complexes **2** and **6** showed no conversion with **S5** at all. Only precatalyst **3** both displayed high conversion (>95%) and selectivity (86%) (Table 3). In summary, dinuclear complexes **1**, **3**, **5** and **7** were in all cases more or at least similarly active (per molecule complex) than mononuclear precatalysts **2**, **4** and **6**. This could, in part, be caused by a dinucleation in presence of adventitious water, resulting in a lowering of the precatalyst loading (per molecule).

Some of the trends observed in epoxidation with TBHP are also valid for epoxidations with H_2O_2, although the overall catalytic activity of precatalysts **1-7** was greatly reduced (Tables 4 and 5). Again complex **3**, in this case together with complex **5**, showed the best performances with H_2O_2, both displaying catalytic activity with four (**S1-2** and **S4-5**) out of the five substrates. Mononuclear complexes **2** and **6** showed no conversion with any substrate, making these two complexes the least active precatalysts out of the seven complexes. In contrast to TBHP epoxidations, also complex **7** remained unproductive in epoxidations of **S1-4** and unselective for **S5**. This lack of catalytic activity with the aqueous oxidant H_2O_2 might be attributed to the enhanced water sensitivity of **7**. Interestingly all seven complexes failed to give any conversion with aromatic substrate styrene **S3** when H_2O_2 was the oxidant (Table 4). In order to rule out a catalase-like activity of precatalysts **1-7**, test reactions under catalytic conditions without added substrate were conducted. The concentration of H_2O_2 was determined after 24 h via iodometric titration, showing that complexes **1-7** do not decompose H_2O_2 under catalytic conditions.

Comparing the TONs (Table 5) allowed the conclusion that dinuclear complexes **3** and **7** exhibited the best overall catalytic activity, being the only two precatalysts showing activity for all five substrates **S1-5** with TBHP as oxidant. Furthermore **3** and **7**, bearing *tert*-butyl and chloride substituents at the phenolate moieties, respectively, gave the highest TONs for **S1**, suggesting a limited influence of the substituents electronic properties on the catalytic activity. However, the increased sensitivity of complex **7** can be attributed to the electron withdrawing nature of the chloride substituents, resulting in a weaker phenolate-Mo bond. From a comparison of the catalytic activities of complexes **3** and **5**, it is evident that the *tert*-butyl substituted dinuclear compound **3** exhibits a better performance over a broader scope of substrates. Whereas this can partly be attributed to the low solubility of complex **5**, it is also possible that the more acidic phenyl-amide moiety is prone to side-reactions such as deprotonation.

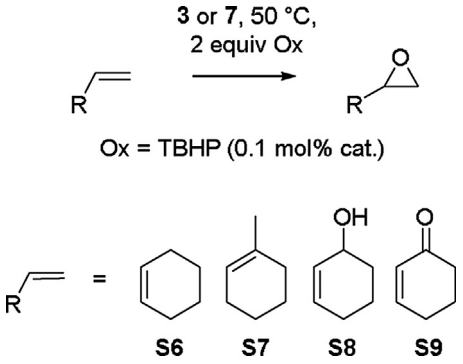

Fig. 4. Epoxidations of olefinic substrates **S6-S9** by complexes **3** and **7.**

For complex **7** the precatalyst loading for **S1** could be even reduced to 0.0005 mol% (5 ppm), giving 54% yield of cyclooctene oxide after 24 h. At 0.001 mol% loading, full conversion of **S1** was obtained within 24 h, indicating a 5 ppm loading of **7** to be the limit of activity. Complex **3** on the other hand showed a remarkable activity with **S5**, hinting towards a high hydroxy functional group tolerance. Also complex **3** showed activity for three out of the five substrates with H_2O_2 as oxidant (Table 4). Taking into account the observed catalytic activities as well as the complexes stability and solubility, precatalysts **3** exhibits the best overall performance.

For these reasons, **3** and **7** were selected for further epoxidation experiments with cyclohexene substrates **S6-S9** (Fig. 4).

Similar to cyclic olefin **S1**, precatalysts **3** and **7** showed high activity and selectivity for substrates cyclohexene **S6** and 1-methyl-1-cylohexene **S7** (Table 6). Whereas especially complex **3** was very tolerant towards the hydroxy group in **S5**, in epoxidation of 2-cyclohexen-1-ol **S8** both **3** and **7** were unselective, oxidizing **S8** to 2-cyclohexen-1-one (**S9**) as the main side product. For **S9** on the other hand, no activity was observed. To further test the tolerance for OH groups, complex **3** and **7** were used for the epoxidation of **S1**

Table 6
Overview of conversion (selectivity to epoxide) of substrates **S6**–**S9**.

	3	7
S6	>95 (>95)	>95 (>95)
S7	>95 (>95)[a]	>95 (>95)[a]
S8	83 (54)	92 (55)
S9	no conv.	no conv.

General conditions: 2 equiv. TBHP (5.5 M in decane), 50 °C, $CHCl_3$, 0.1 mol% precatalyst loading; conversion of substrate (%) after 24 h, as determined by GC–MS (selectivity in% for epoxide in brackets); no conv. = substrate was not converted.
[a] Conversion after 2 h.

Table 7
Overview of conversion of substrate **S1** (selectivity to epoxide) in alcoholic solvents.

entry	precatalyst	loading [mol%]	oxidant	solvent	conversion[a] [%]
1	**3**	1	H_2O_2	EtOH	49 (>95)
2	**3**	1	TBHP	EtOH	75 (90)
3	**3**	0.1	TBHP	MeOH	63 (>95)
4	**3**	0.1	TBHP	EtOH	59 (93)
5	**3**	0.1	TBHP	*i*PrOH	75 (90)
6	**3**	0.1	TBHP	*t*BuOH	89 (95)

General conditions: 2 equiv. oxidant, 50 °C.
[a] Conversion of substrate (%) after 24 h, as determined by GC–MS (selectivity in% for epoxide in brackets).

in ethanol as solvent with TBHP as well as H_2O_2 as oxidant. Whereas **7** showed no activity in ethanol, **3** gave conversion to epoxide with both oxidants (Table 7). Encouraged by this result we tested **3** in the four different alcohols methanol, ethanol, isopropanol and *tert*-butanol.

Precatalyst **3** is active for the epoxidation of substrate **S1** in all four tested alcoholic solvents (Table 7). With the aqueous oxidant H_2O_2, precatalyst activity was lower than compared to TBHP under the same reaction conditions (entry 1 and 2). In contrast to the standard solvent $CHCl_3$, a single phase is formed in the reaction mixture, indicating that the lower activity with H_2O_2 cannot be solely attributed to a miscibility problem between precatalyst, oxidant and substrate. The activity of **3** in MeOH and EtOH is essentially the same (within experimental error), with conversions of 63 and 59% respectively, for **S1** (Table 7, entry 3 and 4). We could demonstrate that complex **4** is formed upon dissolution of **3** in methanol (Scheme 4). Based on the similar pKa value of EtOH (29.8) [26] and MeOH (29.0) [26] the formation of an analogous ethoxido complex is possible, hence explaining the similar catalytic activity. However, an induction period was only observed employing methanol as solvent (Fig. S5). The lack of conversion during the first hour of catalysis indicates the formation of the methoxido species **4** prior to formation of the catalytic active species. Epoxidations in isopropanol and *tert*-butanol show higher catalytic activity (75 and 89% conversion of **S1**, entry 5 and 6), despite the fact that *tert*-butanol is known to be an inhibitory by-product in epoxidations with TBHP as oxidant [18,28]. Mononuclear methoxido complexes **2, 4** and **6** have proven to be less active in epoxidation compared to their dinuclear congeners **1, 3, 5** and **7**, suggesting that the dinuclear complexes are stable in isopropanol or *tert*-butanol and are not cleaved to the corresponding mononuclear alkoxido complexes (*vide supra*).

Significant differences in catalytic activity of dinuclear compared to mononuclear precatalysts suggest a difference in the active catalyst species formed. We have no spectroscopic evidence for a cleavage of the dinuclear compounds in $CHCl_3$, the standard solvent used in epoxidations. Thus, in presence of 10 equiv. TBHP dinuclear complex **3** remains unchanged as shown by ^{1}H NMR spectroscopy, indicating high stability of the complex under oxidative conditions (*vide supra*, Fig. S3). Based on this experimental evidence retention of the dinuclear structure during catalysis is suggested and thus also a different catalytically active species for mononuclear and dinuclear complexes. Furthermore, the high activity in *tert*-butanol is especially surprising, as *tert*-butanol usually impedes epoxidation activity with many other published precatalysts [18,28]. In comparison with structurally related, previously reported μ-oxido bridged complexes (bearing hydrogen bond acceptor functionalities such as —OMe and —NMe_2) [18], the high activity and functional group tolerance of the complexes herein clearly suggest a beneficial role of the additional hydrogen bond donors on the ligand amide functionalities, which seems to be able to stabilize the oxidant and/or substrate molecules in the second coordination sphere. Another benefit of the presented system might be the increased lability of the donor arm, allowing for the formation of a vacant coordination site. It remains unclear however, whether both molybdenum centers in dinuclear complexes **1, 3, 5** and **7** are active in epoxidation catalysis or not.

4. Conclusions

The synthesis of four novel aminophenolate ligands **HL1**–**HL4** with *tert*-butyl and phenyl amide functionalities as hydrogen bond donors is reported. Upon reaction with the molybdenum(VI) precursor [$MoO_2(acac)_2$], they form, dependent on the used solvent, mono- and dinuclear complexes **1**-**7** of the general formulas [{MoO_2**L**}$_2$(μ-O)] and [MoO_2**L**(OMe)], respectively, coordinated by one facially, tridentate ONO-ligand moiety per metal center.

Especially dinuclear complexes **1**, **3**, **5** and **7** were found to be highly efficient and stable precatalysts in the epoxidation of various olefins, leading to turnover numbers up to 110000 with precatalysts loadings of 5–10 ppm, although a lack of chemoselectivity due to over-oxidation was observed for some substrates. The complexes furthermore showed a remarkable tolerance towards hydroxy functionalities as well as moisture, allowing for the use of aqueous H_2O_2 as oxidant as well as alcoholic solvents such as EtOH and thus environmentally benign, "green", reaction conditions in catalysis. Furthermore also catalytic experiments in *t*BuOH (a by-product in epoxidations with TBHP, usually postulated to inhibit the reaction [18,28]) led to high epoxide yields with TBHP (0.1 mol% precatalyst). The high activity and tolerance of the complexes is remarkable in comparison with previously reported, structurally similar compounds with acceptor functionalities (—OMe and —NMe_2), which exhibited negligible activity in alcoholic solvents and/or with H_2O_2 as oxidant. Furthermore the system described herein allowed for the reduction of the precatalyst loading for all tested substrates by at least a factor of 10 [18]. These findings underline the significant benefit of the introduction of hydrogen bond donor functionalities in epoxidation catalysis and therefore clearly warrant a further exploration and implementation in systems for efficient and "green" homogeneous epoxidation catalysis.

Acknowledgements

Financial support by the Austrian Science Fund (FWF, grant number P26264) and NAWI Graz is gratefully acknowledged.

Appendix A. Supplementary data

Supplementary data associated with this article can be found, in the online version, at http://dx.doi.org/10.1016/j.mcat.2017.09.036.

References

[1] J.M. Brégeault, J. Chem. Soc. Dalton Trans. (2003) 3289–3302.

[2] (a) F. Cavani, J.H. Teles, ChemSusChem 2 (2009) 508–534;
(b) T. Endo, A. Sudo, J. Polym. Sci. A Polym. Chem. 47 (2009) 4847–4858.
[3] S. Huber, M. Cokoja, F.E. Kühn, J. Organomet. Chem. 751 (2014) 25–32.
[4] A.K. Yudin, Aziridines and Epoxides in Organic Synthesis, Wiley-VCH, Weinheim, 2006.
[5] H. Adolfsson, D. Bellus, C.J. Forsyth, J. Houben, T. Weyl, Ethers, Thieme, Stuttgart, 2008.
[6] (a) Q.-H. Xia, H.-Q. Ge, C.-P. Ye, Z.-M. Liu, K.-X. Su, Chem. Rev. 105 (2005) 1603–1662;
(b) B.S. Lane, K. Burgess, Chem. Rev. 103 (2003) 2457–2474;
(c) K.C. Gupta, A.K. Sutar, Coord. Chem. Rev. 252 (2008) 1420–1450;
(d) H. Srour, P. Le Maux, S. Chevance, G. Simonneaux Coord, Chem. Rev. 257 (2013) 3030–3050;
(e) J.-E. Bäckvall (Ed.), Modern Oxidation Methods, Wiley-VCH Verlag GmbH & Co. KGaA, Weinheim, Germany, 2010;
(f) K.A. Jørgensen, Chem. Rev. 89 (1989) 431–458;
(g) H. Adolfsson, D. Balan, in: A.K. Yudin (Ed.), Aziridines and Epoxides in Organic Synthesis, Wiley-VCH Verlag GmbH & Co. KGaA, Weinheim, FRG, 2006.
[7] M.G. Clerici, M. Ricci, G. Strukul, in: G.P. Chiusoli, P.M. Maitlis (Eds.), Metal-catalysis in Industrial Organic Processes, Royal Society of Chemistry, Cambridge, 2006.
[8] R.M. Bullock, Catalysis Without Precious Metals, Wiley-VCH, Weinheim, 2010.
[9] L.M. Peschel, J.A. Schachner, F. Belaj, N.C. Mösch-Zanetti, Eur. J. Inorg. Chem. (2017) 2808–2817.
[10] (a) M. Bagherzadeh, L. Tahsini, R. Latifi, L.K. Woo, Inorg. Chim. Acta 362 (2009) 3698–3702;
(b) F.E. Kühn, A.M. Santos, M. Abrantes, Chem. Rev. 106 (2006) 2455–2475;
(c) J.A. Schachner, P. Traar, C. Sala, M. Melcher, B.N. Harum, A.F. Sax, M. Volpe, F. Belaj, N.C. Mösch-Zanetti, Inorg. Chem. 51 (2012) 7642–7649;
(d) J. Pisk, B. Prugovečki, D. Matković-Čalogović, R. Poli, D. Agustin, V. Vrdoljak, Polyhedron 33 (2012) 441–449;
(e) J. Pisk, D. Agustin, V. Vrdoljak, R. Poli, Adv. Synth. Catal. 353 (2011) 2910–2914;
(f) N. Morlot, D. Uyttebroeck, ChemCatChem 5 (2013) 601–611;
(g) I. Sheikhshoaie, A. Rezaeifard, N. Monadi, S. Kaafi, Polyhedron 28 (2009) 733–738;
(h) A. Rezaeifard, I. Sheikhshoaie, N. Monadi, M. Alipour, Polyhedron 29 (2010) 2703–2709;
(i) M. Bagherzadeh, R. Latifi, L. Tahsini, V. Amani, A. Ellern, L.K. Woo, Polyhedron 28 (2009) 2517–2521;
(j) J.M. Sobczak, J.J. Ziółkowski, Appl. Catal. A 248 (2003) 261–268;
(k) J. Zhao, X. Zhou, A.M. Santos, E. Herdtweck, C.C. Roma˜o, F.E. Kühn, Dalton Trans. (2003) 3736–3742;
(l) Y. Sui, X. Zeng, X. Fang, X. Fu, Y. Xiao, L. Chen, M. Li, S. Cheng, J. Mol. Catal. A: Chem. 270 (2007) 61–67.
[11] P. Traar, J.A. Schachner, B. Stanje, F. Belaj, N.C. Mösch-Zanetti, J. Mol. Catal. A: Chem. 385 (2014) 54–60.
[12] J.W. Kück, R.M. Reich, F.E. Kühn, Chem. Rec. 16 (2016) 349–364.
[13] (a) C. Müller, N. Grover, M. Cokoja, F.E. Kühn, Advances in Inorganic Chemistry, Elsevier, 2013;
(b) N. Grover, A. Pöthig, F.E. Kühn, Catal. Sci. Technol. 4 (2014) 4219–4231;
(c) S.M. Bruno, S.S. Balula, A.A. Valente, F.A. Almeida Paz, M. Pillinger, C. Sousa, J. Klinowski, C. Freire, P. Ribeiro-Claro, I.S. Gonçalves, J. Mol. Catal. A: Chem. 270 (2007) 185–194;
(d) M. Abrantes, A.M. Santos, J. Mink, F.E. Kühn, C.C. Roma˜o, Organometallics 22 (2003) 2112–2118;
(e) M.E. Judmaier, C. Holzer, M. Volpe, N.C. Mösch-Zanetti, Inorg. Chem. 51 (2012) 9956–9966.
[14] (a) M.G. Clerici, O.A. Kholdeeva (Eds.), Liquid Phase Oxidation via Heterogeneous Catalysis, John Wiley & Sons, Inc, Hoboken, New Jersey, 2013;
(b) G. Grigoropoulou, J.H. Clark, J.A. Elings, Green Chem. 5 (2003) 1–7.
[15] (a) N. Zwettler, M.E. Judmaier, L. Strohmeier, F. Belaj, N.C. Mösch-Zanetti, Dalton Trans. 45 (2016) 14549–14560;
(b) A. Dupé, M.E. Judmaier, F. Belaj, K. Zangger, N.C. Mösch-Zanetti, Dalton Trans. 44 (2015) 20514–20522;
(c) K. Most, S. Köpke, F. Dall'Antonia, N.C. Mösch-Zanetti, Chem. Commun. (2002) 1676–1677;
(d) G. Lyashenko, G. Saischek, M.E. Judmaier, M. Volpe, J. Baumgartner, F. Belaj, V. Jancik, R. Herbst-Irmer, N.C. Mösch-Zanetti, Dalton Trans. (2009) 5655–5665;
(e) G. Lyashenko, A. Saischek, R. Herbst-Irmer, N.C. Mösch-Zanetti, Chem. Commun. (2007) 701–703;
(f) M. Volpe, N.C. Mösch-Zanetti, Inorg. Chem. 51 (2012) 1440–1449;
(g) N.C. Mösch-Zanetti, D. Wurm, M. Volpe, G. Lyashenko, B.N. Harum, F. Belaj, J. Baumgartner, Inorg. Chem. 49 (2010) 8914–8921;
(h) K. Most, J. Hoßbach, D. Vidovic, J. Magull, N.C. Mösch-Zanetti, Adv. Synth. Catal. 347 (2005) 463–472;
(i) N. Zwettler, N. Grover, F. Belaj, K. Kirchner, N.C. Mösch-Zanetti, Inorg. Chem. 56 (2017) 10147–10150.
[16] (a) N. Zwettler, J.A. Schachner, F. Belaj, N.C. Mösch-Zanetti, Inorg, Chem. 53 (2014) 12832–12840;
(b) N. Zwettler, J.A. Schachner, F. Belaj, N.C. Mösch-Zanetti, Inorg. Chem. 55 (2016) 5973–5982;
(c) P. Traar, J.A. Schachner, L. Steiner, A. Sachse, M. Volpe, N.C. Mösch-Zanetti, Inorg. Chem. 50 (2011) 1983–1990.
[17] A. Dupé, M.K. Hossain, J.A. Schachner, F. Belaj, A. Lehtonen, E. Nordlander, N.C. Mösch-Zanetti, Eur. J. Inorg. Chem. (2015) 3572–3579.
[18] M.E. Judmaier, C.H. Sala, F. Belaj, M. Volpe, N.C. Mösch-Zanetti, New J. Chem. 37 (2013) 2139.
[19] M.E. Judmaier, C. Holzer, M. Volpe, N.C. Mösch-Zanetti, Inorg. Chem. 51 (2012) 9956–9966.
[20] (a) T. Taguchi, R. Gupta, B. Lassalle-Kaiser, D.W. Boyce, V.K. Yachandra, W.B. Tolman, J. Yano, M.P. Hendrich, A.S. Borovik, J. Am. Chem. Soc. 134 (2012) 1996–1999;
(b) R.L. Shook, S.M. Peterson, J. Greaves, C. Moore, A.L. Rheingold, A.S. Borovik, J. Am. Chem. Soc. 133 (2011) 5810–5817;
(c) C.E. MacBeth, A.P. Golombek, V.G. Young Jr., C. Yang, K. Kuczera, M.P. Hendrich, A.S. Borovik, Science 289 (2000) 938–941;
(d) S.A. Cook, E.A. Hill, A.S. Borovik, Biochemistry 54 (2015) 4167–4180;
(e) S.A. Cook, A.S. Borovik, Acc. Chem. Res. 48 (2015) 2407–2414.
[21] N. Zwettler, A. Dupé, J.A. Schachner, F. Belaj, N.C. Mösch-Zanetti, Inorg. Chem. 54 (2015) 11969–11976.
[22] (a) S.A. Hauser, M. Cokoja, F.E. Kühn, Catal. Sci. Technol. 3 (2013) 552;
(b) A. Schmidt, N. Grover, T.K. Zimmermann, L. Graser, M. Cokoja, A. Pöthig, F.E. Kühn, J. Catal. 319 (2014) 119–126;
(c) D. Betz, A. Raith, M. Cokoja, F.E. Kühn, ChemSusChem 3 (2010) 559–562.
[23] (a) F.P. Byrne, S. Jin, G. Paggiola, T.H.M. Petchey, J.H. Clark, T.J. Farmer, A.J. Hunt, C. Robert McElroy, J. Sherwood Sustain. Chem. Process 4 (2016) 1034;
(b) C. Capello, U. Fischer, K. Hungerbühler, Green Chem. 9 (2007) 92.
[24] H. Gehrke, J. Veal Inorg, Chim. Acta 3 (1969) 623–627.
[25] G.M. Sheldrick, Acta Crystallogr., Sect. A: Found. Crystallogr. 64 (2008) 112–122.
[26] W.N. Olmstead, Z. Margolin, F.G. Bordwell, J. Org. Chem. 45 (1980) 3295–3299.
[27] J.M. Mayer, Inorg. Chem. 27 (1988) 3899–3903.
[28] S. Gago, P. Neves, B. Monteiro, M. Pessêgo, A.D. Lopes, A.A. Valente, F.A. Almeida Paz, M. Pillinger, J. Moreira, C.M. Silva, et al., Eur. J. Inorg. Chem. (2009) 4528–4537.